CHAPTER-III

A fast and additive free C-C homo/cross-coupling reaction in reverse micellar gallows: A brief understanding on role of surfactant, water content and base on the yield of the product and possible reaction site therein

III.A. Introduction

Biaryls are important structural motifs, available in various natural products, ligands, drug molecules and functional materials. Various distinct classes of therapeutic molecules are containing biaryl framework.[1] Biaryls are also known to have potential as antitumor, [2] and antihypertensive agents.[3] Several synthetic methods have been developed so far for the construction of biaryl skeletons through C–C coupling reactions. The field of C-C homo/cross coupling reactions is dominated by palladium catalyst. [4-11] Use of additive is very common in palladium catalyzed homocoupling reaction of arylboronic acid. In addition to the palladium (Pd) catalysis, some gold (Au)[12,13] copper (Cu)[14] and manganese [Mn(III)][15] catalyzed homocoupling reactions of arylboronic acids have also been reported. But the common problems associated with these methods are high temperature and long reaction time.[12] In view of these, search to find out a suitable medium for studying these types of reactions is warranted.

Reverse micelles (RMs) can execute as an excellent biomimetic model since it provide local hydrophilic moiety in an organic phase resembling to biological membranes of the amphiphilic phospholipids. The water pool of the RM provides a compartmentalized environment with properties considered to be similar to those found at polar/non-polar interfaces in vivo.[16] In the confined region, free movement of water molecules is restricted and the three-dimensional hydrogen-bonded network is disrupted.[17]The dynamics of confined water in the vicinity of biomacromolecules are believed to be responsible for many biological functions, such as molecular recognition and enzymatic catalysis.[18] In view of these, RMs are reported to be used as microreactors to study a variety of organic reactions[19-22] and yield of the product(s) depend on the type of surfactant used, also on the nature of confinement in RMs.[19-21] Thus, the task specific RMs can, therefore, be formulated by judicious selection of the ingredients. Very recently, we have reported the Pd-NHC catalyzed Heck reaction in

ionic liquid based w/o non-ionic microemulsions/RMs.[22] Highest yield of the coupled product was obtained where microemulsion formed spontaneously with maximum stability. Sometimes, surfactant monolayer also plays vital role in controlling the reaction dynamics in confined environment by attracting reagents at the interfacial region which was considered as the reaction site.[19-22] Hence, a wide scope prevails to study organic reactions in RMs comprising surfactants with different charge types [*viz*. anionic, AOT, (sodium 1,4-bis(2-ethylhexyl)sulfosuccinate, Na(DEHSS)), cationic, DDAB (didodecyldimethylammonium bromide) and non-ionic TX-100 (t-octylphenoxypolyethoxy ethanol) with variation in configuration of polar head groups and hydrophobic moieties (Scheme-III.1) under varied physicochemical conditions. Cyclohexane (Cy) has been chosen as bulk phase for convenient extraction of the final products.

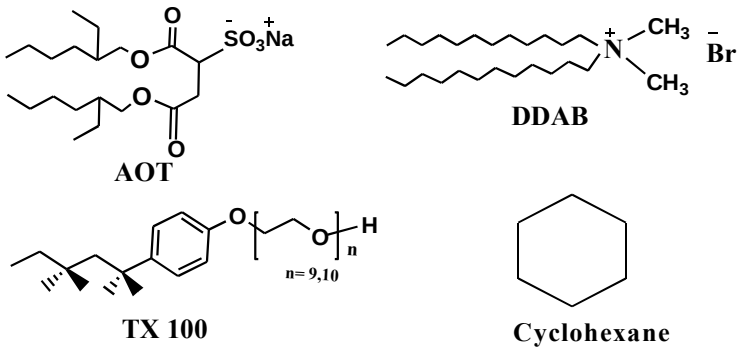

Scheme-III.1. Molecular structure of AOT, DDAB, TX-100 and cyclohexane

This report has been emphasized on the construction of C-C bond with special reference to the transition metal catalyzed additive free C-C homo/cross-coupling reaction of arylboronic acid (herein, phenylboronic acid was selected as a model compound) in these reverse micellar gallows at ambient condition. At the outset, all these RMs (stabilized by surfactants of different molecular structures and physicochemical properties etc. mentioned earlier) have been characterized by employing conductance, DLS and FTIR techniques in order to provide an outline on the performance of the reaction as well as a comparative output of the final product in terms of the yield. Further, a series of studies were undertaken to perform above mentioned reaction in the medium which produces highest yield (herein, AOT/Cy RM) to find out a most suitable base (which is essential for this type of reaction) and also, variation of the yield as a function of water content (ω) under optimized condition. A rationale on the progress of the reaction(s) in constrained environment of AOT RM and the possible reaction site, have also been assessed by employing conductance, DLS and FTIR techniques. Finally, it was contemplated to explore the construction of unsymmetrical biaryl *via* Suzuki-Miyaura

cross-coupling reaction of aryl halides with phenylboronic acid (28 different entries) in AOT RM using same protocol. The yield of coupled products have been discussed in view of variation in electron withdrawing group in arylhalides (Cl^-, Br^- and I^-) and bond strength between C-halides.

II.B. Results and Discussion

Before going to discuss about the construction of C-C bond and design of different organic motif through the transition metal catalyzed additive free C-C homo/cross-coupling reaction in reverse micellar media at ambient condition, first we emphasize on the microstructural and microenvironmental characteristics of the templates viz. anionic, cationic and non-ionic surfactant based reverse micelles (RMs).

II.B.1. Formation and Characterization of anionic, cationic and non-ionic RMs

The anionic surfactant, AOT, cationic, DDAB and nonionic TX-100 are well-known emulsifiers and envisioned for the formulation of RMs in cyclohexane by exploiting the same.[7-12] All the measurements were performed at a fixed surfactant concentration, [S_T] of 0.5 mol dm^{-3} at 303K.

II.B.1.1.Conductivity measurement

Electrical conductivity is a structure sensitive property of water-in–oil (w/o) microemulsion/RMs. The existence of microstructural regimes, namely spherical droplets and aggregated clusters, can be predicted from the nature of the plots.[23] Figure-III.1. (A, B and C) shows the variation of electrical conductivity as a function of water content (ω) for AOT/Cy, DDAB/Cy and TX-100/Cy RMs, respectively at 303K.

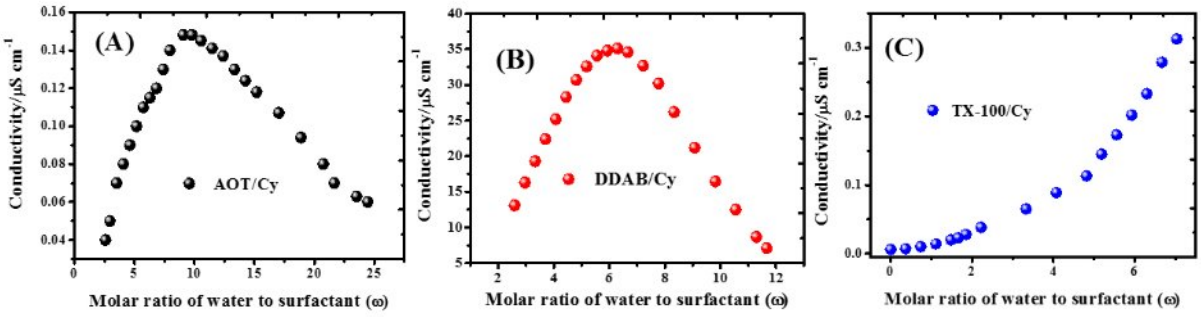

Figure-III.1. The variation of electrical conductivity a function of water content (ω) for AOT (A), DDAB (B) and TX-100 (C) RMs, respectively in cyclohexane (Cy) at 303K.

It can be seen in Figure-III.1. A, the conductivity of AOT/Cy RM increases upon increasing ω at the initial stage. After reaching a maximum (at ω= 10), it decreases until phase separation. The low-conductance behavior and also, a maximum in conductivity in this medium can be explained as follows:[24,25] At low water content, the solubilized water molecules, which are mainly encapsulated in nanosized domains, are preferably involved in ion hydration and associate to Na^+ and head groups tightly. Some of these Na^+ ions bind to the surfactant reside in close proximity of the oil/water interface or palisade layer and hence, they are immobilized, which makes the aqueous environment quite rigid. The surfactant aggregates approach and fuse to form a short-lived dimer and subsequently, they separate to form two new isolated droplets. During this process, the counter ions randomly redistribute and give rise to separately charged droplets, which migrate in the oil-rich medium under an electrical field and result in the low conductance.[26, 27]The appearance of maximum in conductivity is an outcome of several antagonistic effects that influence the conductance behaviors of the system. The added water tends to form water pools in the cores of nanodroplets as the water content exceeds the demand for hydrating surfactant headgroups and counter ions. With increase in water solubilization, the hydrated counter ions exchange and redistribute readily during the process of droplet collision and transient fusion, which contributes to the increase in conductivity.[27] An analogous variation in conductance i.e. appearance of bell-shaped curve with a maximum in conductivity (at ω= 6), has been observed for DDAB/Cy RM as a function of ω, as shown in Figure-III.1.B and can be attributed to charge fluctuation.[28] The conductivity of DDAB RMs show higher values than that of AOT based RM and the maxima in conductance occur at lower water content (ω) (Figure-III.1.A and B). Different types of (i) polar head groups and counter ions of AOT ($DEHSS^-/Na^+$) and DDAB ((DDA^+/Br^-), (ii) size of polar head groups (55 A^{02} for AOT/ 68 A^{02} for DDAB) and (iii) penetration of their polar head groups inside the water pool and constitution of the interface *vis-a-vis* its flexibility or rigidity might be effective for above variation in conductance.[29, 30] However, TX-100/Cy RM shows gradual increase in conductivity with increase in ω. However, no maximum in conductivity was observed even at high water content (in the presence of 0.9 % NaCl) till phase separation,[31] as illustrated in Figure-III.1. C. This reflects a regular buildup of an infinite network containing connected or fused droplets in TX-100 RMs.

III.B.1.2. Dynamic light scattering measurement

A DLS experiment allows the droplet size determination of the RMs, and is also, competent to identify populations with distinct size distributions, and therefore, reveals the presence/formation of aggregates.[32] In view of this, the size and size distributions of RM droplets are measured by DLS technique. Figure-III.2 (A, B) depicts the variation of droplet size and droplet count rate for AOT, DDAB and TX-100 based RMs in cyclohexane as a function of water content (ω) at a fixed temperature (303K). The hydrodynamic diameter (D_h) of RM droplet increases with increase in water content (ω) for all the RMs whereas decrease of the droplet count rate has been observed under the prevailing condition, keeping other parameters constant [Figure-III.2 (A, B)]. Bardhan et al. reported that the droplet count rate is directly proportional to the droplet number of the RMs.[33, 34] Hence, it clearly indicates the swelling behaviour of RMs and aggregation of smaller droplets into large one and thereby, increases the droplet size and decreases the droplet number with the addition of water. Further, the results clearly indicated that D_h follows the order: $RM_{AOT} < RM_{DDAB} < RM_{TX\text{-}100}$ at comparable ω (up to 7.0) whilst droplet count rate shows reverse trend [Figure-III.2 (A, B)].

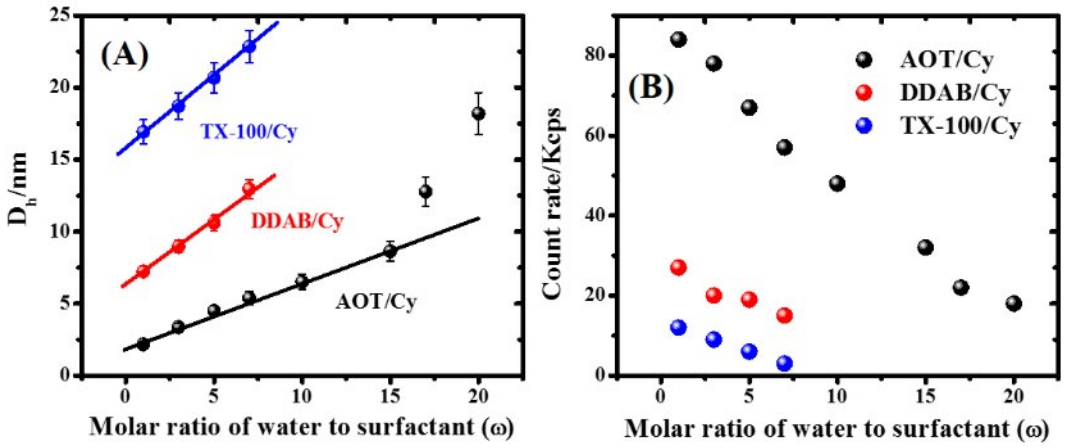

Figure-III.2. The variation of droplet size (A) and droplet count rate and (B) for AOT, DDAB and TX-100-Cy blended RMs as a function of water content (ω) at a fixed temperature (303K).

The droplet size of RMs depends, among many other variables, on the surfactant packing parameter (P).[23] Such phenomena could be attributed to the variation in an effective packing parameter of surfactant, v/al_c, in which v and l_c are the volume and the length of the

hydrocarbon chain, respectively, and *a* is the head group area of surfactant.[27, 35, 36] It is noteworthy that the polar head group area (*a*) of the nonionic surfactant (herein, TX-100) is larger than that of cationic (DDAB) and/or anionic (AOT) surfactant as nonionic surfactant possesses long polyoxyethylene chain (9/10-POE chains) as polar head thereby decrease the value of effective packing parameter (P).[37,38] It gives rise to an increase in radius of the droplets in nonionic RMs (herein, TX-100).[27, 33] It can be inferred that variation in D_h of these RMs depends on type and size of polar head groups and hydrophobic moieties of surfactant (AOT, DDAB and TX-100), which influence the formation of reverse aggregates (Figure-III.2 A). Moreover, the linear variation of droplet size as function of ω indicates that the droplets do not interact each other and are probably spherical. The deviation from linearity as evident for AOT RMs at higher ω value (> 10) is due to several factors. Of these, the most relevant one being enhanced droplet-droplet interaction and shape of the RMs.[39]

III.B.1.3. FTIR spectroscopy

Reports on the properties of the encapsulated water in a range of size and charge type of RMs by studying the states of water organization using FT-IR measurement, are available in literature. [22, 34, 40-43] We have measured mid infrared region (MIR) FTIR spectra for different RMs in cyclohexane as a function of water content (ω) and the temperature (303K). We focus our attention to the 3000−3800 cm^{-1} frequency window as this is a fingerprint region for the symmetric and asymmetric vibrational stretch of O−H bonds in water.[44-46] It is well known that the nanoscopic confinement and droplet size have a strong impact on water hydrogen bond network dynamics regardless of the nature of the interface in RMs. Different types of hydrogen bonded water molecules exist in RMs which can broadly be classified into two major classes, namely, bound and bulk-like water molecules.[40-43] Hence, FTIR spectra of O-H band of water for AOT, DDAB and TX-100 derived RMs have been analyzed and deconvoluted into two peaks at ~3450 and ~3250 cm^{-1}, corresponding to the O-H stretching frequency of the bound and bulk-like water molecules, respectively. A representative result of deconvolution (relative abundance of different water species) is depicted in Figure-III.3 (A, B and C).[40-43]

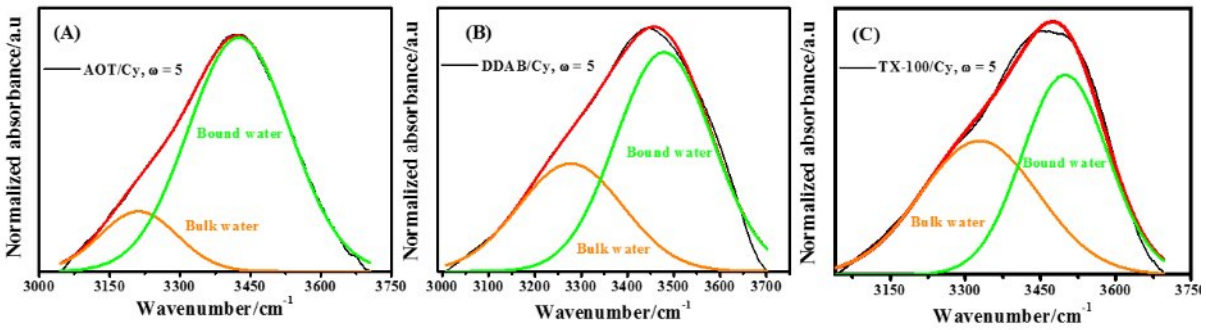

Figure-III.3. Representative normalized (normalized to intensity of 1.0) FTIR spectra of O-H band for AOT (A), DDAB (B) and TX-100 (C)- Cy blended RMs at a fixed water content (ω=5) and temperature (303K). Specification: Experimental spectra (black curve), overall fitted line (red) and deconvoluted curves (bulk water (orange), bound water (green).

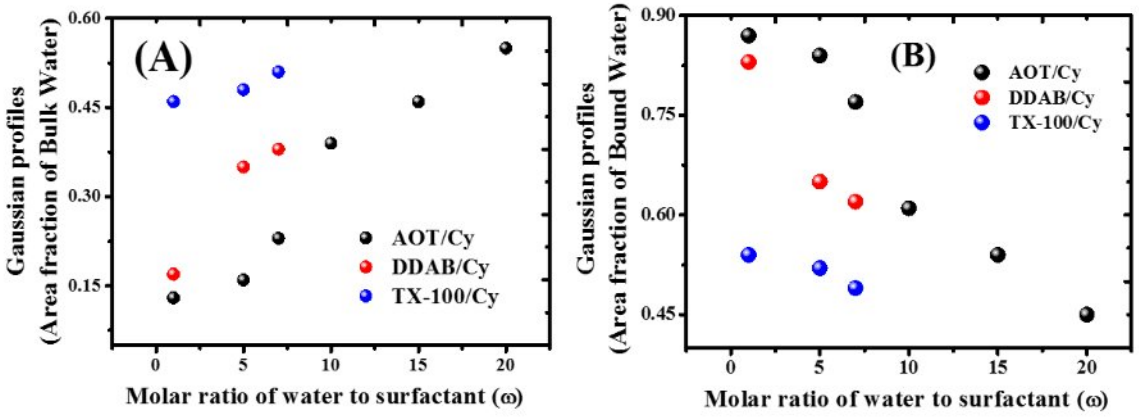

Figure-III.4. The relative abundance [Gaussian profiles (area fraction)] of different water species (bulk (A) and bound (Bound)) in AOT, DDAB and TX-100–Cy blended RMs as a function of ω.

The relative abundance [Gaussian profiles (area fraction)] of different water species in these systems as a function of ω is presented in Figure-III.4. It reveals that the relative abundance of bulk water increases and that of bound water decreases with increasing water content vis-à-vis droplet size (D_h) for all the RMs. Actually, once water is added to a RM forming system, a portion of the water goes to the interface and hydrates the head groups of surfactants till they become fully hydrated at a certain ω. Further addition of water goes primarily to the inner core, leading to a continuous increase in the fraction of unbounded free bulk like water with increase in ω.[47] Interestingly, it reveals from Figure-III.3 and 4 that the bound water proportion is the least in TX-100 formed RMs. Whereas, the proportion of bound water increases in presence ionic surfactant (AOT or DDAB) derived RMs and

follows the order: $RM_{TX\text{-}100} < RM_{DDAB} < RM_{AOT}$. These results indicate a significant role of surfactant charged types and polar head group in determining the proportion of different water species (bound and bulk) in the confined environment of RMs. Uncharged head group nonionic surfactant (herein, POE chain of TX-100) interacts less strongly with the water molecules as does the ionic surfactant head groups (DDAB and AOT), thereby decreasing the population of bound type water molecules in TX-100 formed RMs.[48] Further, the surface area per AOT head group is larger, leading to its interactions with more water molecules and increased water penetration at the interface of AOT RMs leading to water-ester interactions by intermolecular H-bonding vis-à-vis highest bound water population.[49] It is noteworthy that lowest D_h of AOT RMs also subsidizes the highest bound water population as decreasing droplet size increases the bound water proportion in RMs and vice versa.[22, 33, 34]

III.B.2. Standardization of Homocoupling reaction

In preceding paragraphs, AOT, DDAB and TX-100 RMs in cyclohexane show considerable difference in physicochemical characteristics which depend on the charge types, configuration of polar head groups and hydrophobic moieties of surfactant under varied conditions, as evident from conductivity, DLS and FTIR measurements. In view of all these aspects an attempt has been made to compare the effect of different types of RMs on the reaction yield and also, to find out the best combination of RM medium and the base required for effective C-C homocoupling reaction of arylboronic acid which is albeit a major part of presentation of this section. Herein, phenylboronic acid was selected as a model compound for homocoupling reaction.

Triton X-100 RMs in cyclohexane can solubilize maximum amount of water only up to ω (molar ratio of water to surfactant) equals to 7 at a fixed surfactant concentration, $[S_T]$ of 0.5 mol dm^{-3}. Hence, identical hydration level and $[S_T]$ of other two surfactants (viz. AOT and DDAB) has been chosen to underline the comparative efficacy and the corresponding results are summarized in Table-III.1.

Table-III.1. Optimization of reaction condition for homocoupling reaction in RMs[a]

Entry	Solvent	ω	Base	Yield(%)[d]
1	Cy[b]	——	K_2CO_3	50
2	H_2O[b]	——	K_2CO_3	62
3	Water/TX-100/Cy[c]	7	K_2CO_3	64
4	Water/DDAB/Cy[c]	7	K_2CO_3	75
5	Water/AOT/Cy[c]	7	K_2CO_3	81
6	Water/AOT/Cy[c]	5	K_2CO_3	73
7	Water/AOT/Cy[c]	10	K_2CO_3	88
8	Water//AOTCy[c]	15	K_2CO_3	91
9	Water/AOT/Cy[c]	20	K_2CO_3	82
10	Water/AOT/Cy[c]	15	Na_2CO_3	86
11	Water/AOT/Cy[c]	15	Cs_2CO_3	96
12	Water/AOT/Cy[c]	15	K_3PO_4	93
13	Water/AOT/Cy[c]	15	——	86
14[e]	Water/AOT/Cy[c]	15	Cs_2CO_3	<10

[a]Reaction Condition: Phenylboronic acid (1 mmol), base (2 mmol), $Pd(OAc)_2$ (2 mol%), Solvent (3 ml); [b]Reaction was continued for overnight; [c]Water/surfactant/oil, RM contains 1 mmol surfactant and 2 ml oil in each case; [d]Isolated Yield; [e]$Cu(OTf)_2$ was used as catalyst.

Both nonionic TX 100 and cationic DDAB based RMs responded well and resulted in good yield (64% and 75%, respectively) of desired homo-coupled product (Table-III.1; entry 3, 4). However, highest yield (81%) was obtained in presence of anionic AOT under identical condition. In addition, the yields of the product are also measured in the constituents of these formulations as media (Table-III.1; entries 1, 2). Both water and cyclohexane results in low yield compared to RM, Hence, it may be concluded that AOT, DDAB and TX-100 surfactants are quite competent to tune the architecture of RMs starting from the interfacial film to the confined environment (water pool) in a different way due to their inherent characteristics and subsequently, effect the reaction yield at comparable physicochemical condition.[34, 50]

For example, DDAB is essentially insoluble in pure oil, and the small amount water required to form reverse micelle is believed to solvate the head groups and counterion, and beyond which phase separation occurs. Further, because of its poor solubility in water and oil too, it is reported that DDAB molecules are predominantly adsorbed at the oil/water interface and results in less flexible (rigid) so that penetration of the bulkier headgroups (cationic, DDA^+) into the water pool makes difficult. (Scheme-III.1).[51,52] On the other hand, AOT has received much larger attention to form RM due to its ability to solubilize large amounts of water in a variety of nonpolar solvents over a wide range of concentrations. Its special structural characteristics (Scheme-III.1) reveal formation of a more flexible interface so that a comparable less dimension of polar headgroups (anionic, $DEHSS^-$) can protrude towards water pool more easily.[53] Whereas, TX 100 contains polyoxyethylene (POE) group as a hydrophobic part (polar head group), which may be larger than the hydrophobic part of the molecule. Because of the presence of long POE group, polar interior of reverse micellar aggregates thus formed, has shown much different nature from formed with ionic surfactants.[54, 55] Interestingly, the results reveal that AOT is best suited for present study. The low conductivity, small droplet size and high population of bound water species of AOT RMs might be operational for the hike in reaction yield therein. In addition, a plausible explanation in view of the foregoing discussions on difference in characteristic features of microenvironment of the water pool of three RMs can be drawn that

stronger electrostatic interaction between catalyst [$Pd(OAc)_2$] and anionic head group of AOT prevails inside the pool, which corroborates stronger catalytic support to enhance the yield. Whereas, DDAB and TX- 100 do not subscribe any additional support due to difference in microenvironments and microstructures of these RMs emerges from bulkier cationic polar head group (DDA^+) and bulkier POE group (as dipole).

Henceforth, the optimization with respect to other reaction parameters (viz. droplet size, base etc.) has been resolved using AOT based RMs in subsequent sections. The schematic diagram for the homocoupling reaction in AOT based RMs is depicted in Scheme-III.2, which reveals compartmentalization of hydrophilic and lipophilic reactants in water pool and palisade layer of surfactant, respectively separated by the oil/water interface. Size of the aggregated droplets, characterized by ω, affects the local aqueous environments of RMs.[16] Changes in the droplet size of RMs are another proposition to tune the population of amphiphiles at the droplet surface under identical [S_T]. In order to compare the effect of encapsulation or compartmentalization of the constituents/reactants in the present reaction with variation of ω (=5→20) vis-à-vis droplet size (D_h =4.49→ 18.20), we have performed model reaction in water/AOT/cyclohexane RMs and the results are presented in Table-III.1 (Entry-6,7,8,9). It is evident from Table-III.1 that the yield of the desired product increases with ω up to 15 and thereafter, it decreases. More precisely, the highest yield of the desired product (91%) has been observed at ω=15 indicating the finest level of size (D_h =8.64) which facilitates the coupling reaction therein. Hence, it reveals that the different degrees of confinement as a function of ω in water pool can enable to control the reactivity in RMs.[19]

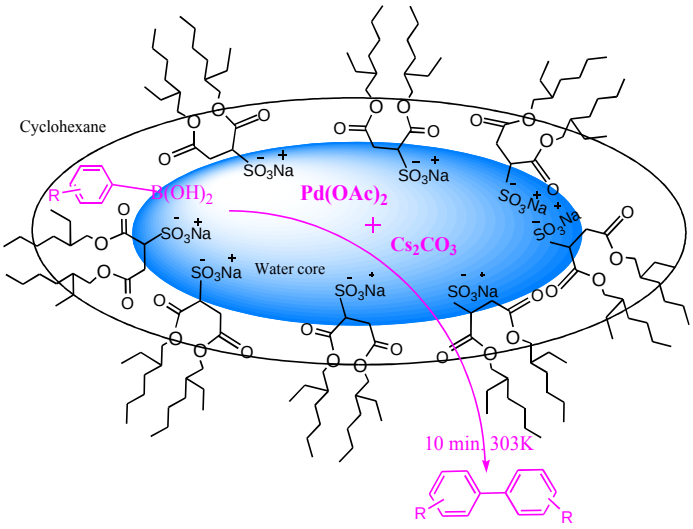

Scheme-III.2: Homocoupling of arylboronic acid in RMs

Among the different bases as enlisted in Table-III.1, highest yield (96%) of the product (Table-III.1; entry-8) was obtained in the presence of Cs_2CO_3 and its superiority to all bases validated under the reaction condition. After optimizing all parameter, we have tested one reaction in presence of $Cu(OTf)_2$, and corresponding result is given in Table-III.1, entry 14. It is cleared from the results that $Pd(OAc)_2$ is better catalyst in comparison to the $Cu(OTf)_2$ for the homocoupling reaction of arylboronic acids.

III.B.3. Growth of reaction in RMs gallows and plausible reaction site therein

From preceding sections, it reveals that AOT/Cy RM has been found to be an effective reaction medium for C-C coupling reactions. The model homocoupling reaction has been performed in this medium and followed by evaluation of different physicochemical properties during proceedings of the reaction to monitor the growth of reaction and accordingly, most plausible reaction location in AOT RM has been deciphered in the following sections.

III.B.3.1.Conductivity measurement

Electrical conductivity of RM has been measured at regular interval during progress of the reaction under optimized condition and the results are presented in Figure-III.5 (A, Table-B.S1). At onset, increase in conductivity upon addition of catalyst $Pd(OAc)_2$ is

obvious but subsequent decrease in conductivity reflecting the formation of non-conducting aqua-palladium complex.[22,56] A sharp increase in conductivity has observed after addition of other reagents and this trend is continued until the completion of reaction. In homocoupling reaction, the product biaryls are formed along with highly conducting side-products [$B(OH)_4^-Cs^+$, $CsHCO_3$] which are responsible for hike in conductivity during reaction.[57] Hence, it can be reasonable to assume that the reaction probably occurring within the droplets of AOT RM.

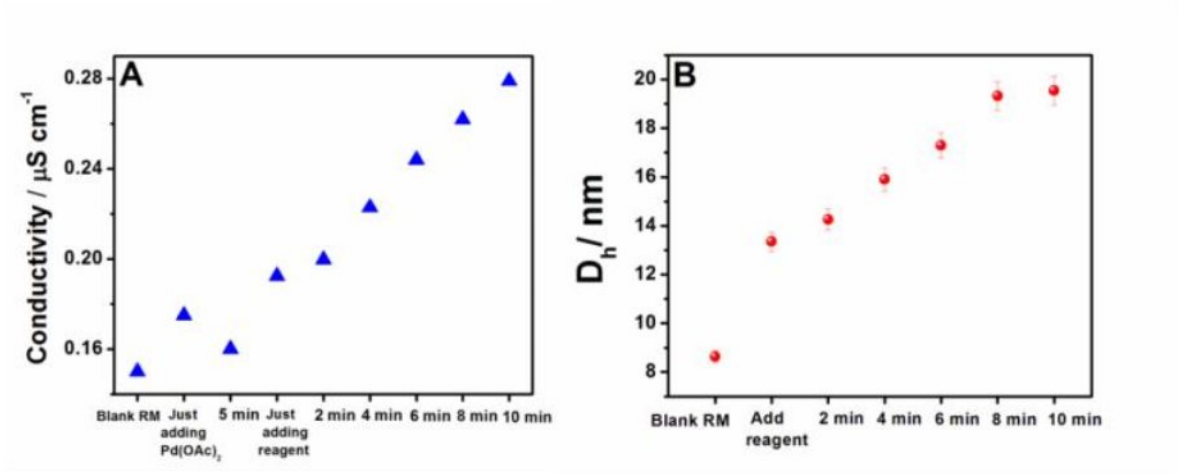

Figure-III.5. (A) The conductivity and (B) the hydrodynamic diameter (D_h) of RMs during course of the reaction.

III.B.3.2.Dynamic light scattering (DLS) measurement

Results of DLS measurement of droplet sizes (D_h) of AOT RMs during course of reaction are presented in Fiure-III.5.B. A sudden increase in D_h (from 8.64 to 13.35 nm) has been observed after addition of reagents, and this trend continues until it reaches to optimal label which actually indicates the end point of reaction. Water soluble reagents [*viz*. catalyst, base mentioned in Table-III.1] get easily solubilized inside the water pool whereas phenylboronic acid, being a sparingly water soluble reagent which possess both hydrophilic and hydrophobic components is expected to be located at the vicinity of oil/water interface of RMs. As a consequence, hydrophilic part of the molecule extends towards water pool due to hydrogen bonding and hydrophobic part obviously incorporates into hydrocarbon domain in the vicinity of the interface/palisade layer.[20, 22] Nevertheless, accumulation of reagents inside water droplets and the presence of phenylboronic acid in the palisade layer of RMs together are responsible for enlargement of droplet size. The regular increase in droplet size during reaction might be due to the formation of the products (both desired and side) and optimal

droplet size reflecting the end of reaction. All these observations together sensing that the reaction takes place inside the water droplets.

III.B.3.3.FTIR measurement

As discussed earlier, the different types of hydrogen bonded water molecules exist in RMs, can broadly be classified into two major classes, namely, bound and bulk-like water molecules [34, 40-43, 58-61] with a characteristic O-H stretching frequency in IR spectroscopy at ~3450 and ~3250 cm^{-1}, respectively (Figure-III.6 and Inset A). Interestingly, the progress of the reaction monitored by FTIR reveals that the addition of palladium acetate initially reduces the population of bound water due to the formation

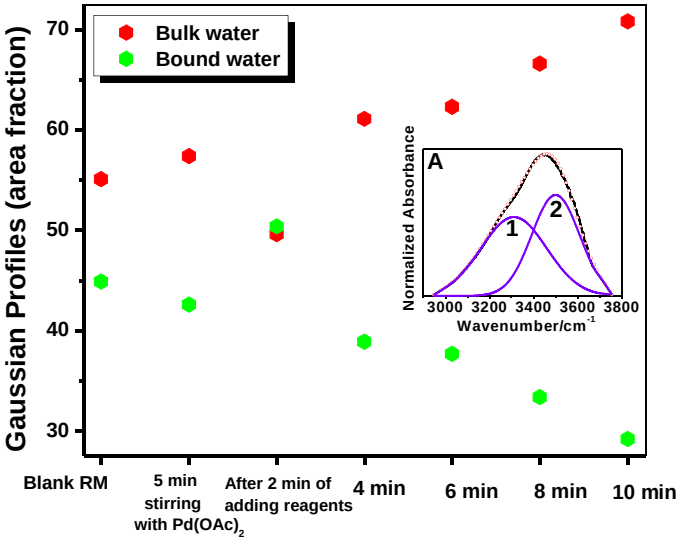

Figure-III.6. The Gaussian Profiles of FTIR study of AOT RMs at regular interval during homocoupling reaction at fixed ω (= 15) and 303 K. Inset A. Representative normalized (normalized to intensity of 1.0) FTIR spectra of O-H band for blank AOT RMs at constant ω (= 15) and 303K. Specification: Experimental spectra (black curve), overall fitted points (red) and deconvoluted curves (1: bulk water; 2: bound water).

of aqua-palladium complex, which decreases the interaction of bound water with polar head groups of AOT. Subsequently, the addition of phenylboronic acid initially enhances the population of bound water as it form H-bond with confined water molecules. Hence, it can be inferred that the molecules of phenylboronic acid essentially reside in the vicinity of the oil/water interface. Thereafter, the bound water population regularly decreases till the completion of reaction. This observation indicated by the formation of biaryls results in

decrease in population of phenylboronic acid at the oil/water interface. Further, the decrease in bound water population may be due to the effect of limiting the interaction between the polar head groups ($DEHSS^-$) of AOT and water.[61] Hence, it can be concluded from overall observations that the reaction takes place in droplets of RMs with special reference to the bound layer of water molecules.

III.B.4.Generalization of AOT RM as reaction media

With this optimized condition presented, an attempt has been made further to establish the versatility of our present protocol. A variety of arylboronic acids were examined under the optimal reaction condition in AOT RMs and the corresponding results/products are summarized in Table-III. 2.

Table-III.2. Homocoupling of different arylboronic acids[a]

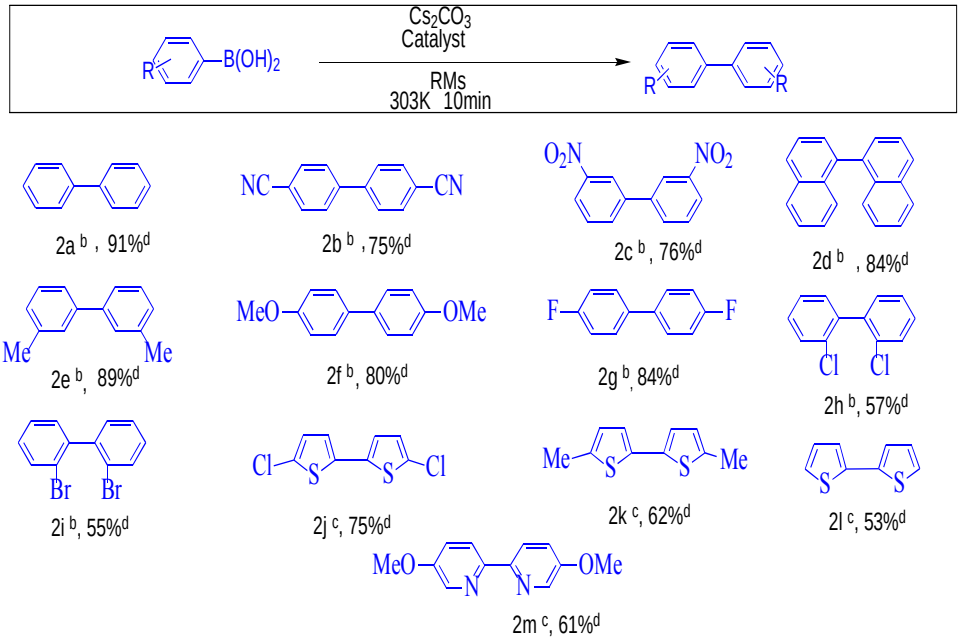

[a]Reaction condition: Arylboronic acid (1mmol); base (2 mmol); catalyst (2 mol%); RMs (3 ml); [b]$Pd(OAc)_2$ used as catalyst; [c]$Cu(OTf)_2$ used as catalyst; [d]Isolated yield after column chromatography.

The reaction progressed smoothly and functional groups were well tolerated under the reaction condition. It is clear from the results that arylboronic acids bearing electron withdrawing groups, (*e.g.,* -Br, -Cl, -F, -CN and $-NO_2$), participate in reactions smoothly and results in good yield of the desired homo-coupled products (Table-III.2; 2b,2c,2g-2i). Arylboronic acids bearing electron-donating groups, (e.g.,-Me and –OMe) furnished the desired products with high yields of 89% and 80%, respectively (Table-III.2; 2e,2f) upon

isolation. *Para* and *meta* substituted arylboronic acids afforded good yields whereas, the dimerisation of *ortho* substituted phenylboronic acids produced the corresponding product with low yields (Table-III.2; 2h,2i), which may be attributed to the steric effect of the substituents present in *ortho* position. Under the same reaction condition, 84% of binaphthyl product was isolated from the naphthylboronic acid (Table-III.2; 2d).

After successful completion of homo-coupling reaction of arylboronic acid, we turned to apply same protocol in case of heteroarylboronic acids. Homo-coupling of heteroarylboronic acid under optimized condition persistently resulted in low yield of the desired product. It might be due to the strong affinity of hetero atom to palladium and accordingly, poisons of the catalyst.[62] We then, modified our protocol and introduced $Cu(OTf)_2$ as catalyst instead of $Pd(OAc)_2$. Under this modified condition, heteroarylboronic acid proficiently responded in homo-coupling reaction and resulted in good yield of the desired product (Table-III.2; 2j-2m).

III.B.4.1.Suzuki cross coupling reaction of aryl halides with phenylboronic acid

In this section, scope of the protocol under investigation was further explored for the construction of unsymmetrical biaryl *via* Suzuki-Miyaura cross-coupling reaction. Accordingly, we have performed a few cross-coupling reactions and results are presented in Table-III.3. Interestingly, the cross-coupling reaction under optimized condition facilitated over homo-coupling reaction and resulted in unsymmetrical biaryl in good to moderate yield. Aryl iodides are ended up with the good yield of cross-coupled product in comparison to arylbromides (Table-III.3).Whereas arylchlorides are not responding in reaction under the optimized condition even after 24 hrs (3l, 3m, 3n).

A slight decrease in product yield for aryl bromides has been observed, and may be due to the higher bond strength of C-Br in comparison with C-I.[63] The presence of electron withdrawing group in arylhalide (Table-III.3, entry 3d, 3g) enhances the yield of the coupled product. The cross-coupled product 1-(3-chlorophenyl)benzene (3j) has been isolated in good yield upon reaction between 1-chloro-3-iodobenzene and phenylboronic acid on selective basis. When 1,3-dibromobenzne treated with phenylboronic acid (2 equivalent) under optimized condition, a decent yield (62%) of 1,3-diphenylbenzene (3k) has been observed.

Table-III.3. Suzuki-Miyaura cross coupling of different Aryl halides with Phenylboronic acid[a]

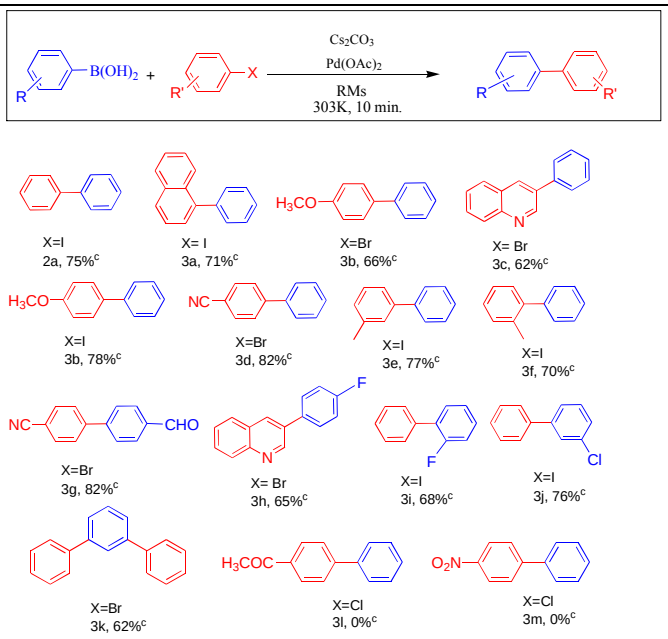

[a]Reaction condition: Arylboronic acid (1mmol); aryl halide (1mmol); base (2 mmol); catalyst (2 mol%); RMs (3 ml); [c]Isolated yield after column chromatography.

III.C. Experimental

III.C.1.Materials and Methods

Dioctyl sulfosuccinate sodium salt (AOT, ≥ 98%, commercial name of the sodium salt of bis(2-ethylhexyl)sulfosuccinate [Na(DEHSS)]), didodecyldimethylammonium bromide (DDAB, ≥ 98%), t-octylphenoxypolyethoxyethanol, palladium acetate [Pd(OAc)2, ≥ 99.98%] arylboronic acids, cesium carbonate, potassium carbonate, palladium acetate, and copper triflate were purchased from Sigma Aldrich, USA. cyclohexane (Cy, ≥ 98%) was the product of Fluka, Switzerland. All these chemicals were used without further purification. Doubly distilled water of conductivity less than 3 μS cm^{-1} was used in the experiments.

Conductivity measurements were performed using Mettler Toledo (Switzerland) Conductivity Bridge. The instrument was calibrated with standard KCl solution. The uncertainty in conductance measurement was within ±1%.

DLS measurements were carried out using Zetasizer Nano ZS90 (ZEN3690, Malvern Instruments Ltd, U.K.). He-Ne laser of 632.8 nm wavelength was used and

the measurements were made at a scattering angle of 90^0. FTIR absorption spectra were recorded in the range of 400-4000 cm^{-1} with a Shimadzu 83000 spectrometer (Japan) using a CaF_2-IR crystal window (Sigma-Aldrich) equipped with Press lock holder with 100 number scans and spectral resolution of 4 cm^{-1}. Deconvolution of spectra has been made using Origin software.

NMR spectra were recorded on 300 MHz spectrometer at 298 K and calibrations were done on the basis of solvent residual peak. Products were isolated using column chromatography on silica gel (60-120 mesh) and a mixture of petroleum ether (60^0-80^0C)/ethyl acetate was used as an eluent. Reaction progress was monitored by silica gel TLC.

III.C.2. General procedure for C-C homo/cross coupling reactions

A 10 ml reaction vial was charged with arylboronic acids (1 mmol), base (2 mmol), catalyst [2 mol%, $Pd(OAc)_2$ for arylboronic acids and $Cu(OTf)_2$ for heteroarylboronic acids]/aryl halide (1 mmol) [only for cross-coupling reaction] and RM (3 mL; $[S_T]$ of 0.5 mol dm^{-3} at 303K). The mixture was stirred at room temperature for 10 minutes. Then the reaction mixture was diluted with water and extracted with dichloromethane (3 x 10 mL). Combined organic layer was dried over anhydrous Na_2SO_4 and concentrated under reduced pressure. The crude residue was purified by silica gel column chromatography using the mixture of petroleum ether and ethyl acetate as eluent.

III.C.3. Spectral analysis

Biphenyl (2a)[64] **:** White solid; mp 68-71°C; 1H NMR ($CDCl_3$, 300 MHz); δ: 7.30–7.35 (m, 2 H), 7.39–7.45 (m, 4 H), 7.56–7.59 (m, 4 H); ^{13}C NMR (75 MHz, $CDCl_3$): δ 127.26, 127.34, 128.85, 141.31.

4,4´-Dicyanobiphenyl (2b)[4] **:** White solid; mp 233-235^{0}C; 1H NMR ($CDCl_3$, 300 MHz) δ : 7.68 (dd, J = 4.8 Hz, 6.6 Hz, 4H), 7.77 (dd, J = 4.8 Hz, 6.6 Hz, 4H); 13C NMR (CDCl3, 75 MHz)δ : 143.4, 132.8, 127.8, 118.3, 112.3.

3,3´-Dinitrobiphenyl (2c)[14] **:***Yellow solid; mp 200-202^{0}C; 1H NMR (CDCl3, 300 MHz) δ : 7.71 (t, J = 7.1Hz, 2H), 7.97 (d, J = 7.5Hz, 2H), 8.31 (d, J = 7.6Hz, 2H), 8.50 (t, J = 1.8Hz, 2H); ^{13}C NMR (CDCl3, 75 MHz) δ: 122.1,123.3,130.3,133.0,140.3,148.8.*

1,1´-Binaphthyl (2d)[15]**:***White solid; mp 141-142^{0}C; 1H NMR ($CDCl_3$, 300 MHz) δ : 7.22-7.29 (m, 2H), 7.40-7.49 (m, 6H), 7.57 (t, J = 7.5Hz, 2H), 7.93 (d, J = 8.4Hz, 4H); 13C NMR ($CDCl_3$, 75 MHz)δ:125.4, 125.8, 126.0, 126.5, 127.8, 127.9, 128.1, 132.8, 133.5, 138.4.*

3,3´-Dimethylbiphenyl (2e)[64]**:***Colourless liquid; bp 286^{0}C; 1H NMR (CDCl3, 300 MHz) δ : 2.46 (s, 6H), 7.19 (d, J = 6.6Hz, 2H), 7.36 (t, J = 7.8Hz, 2H), 7.43 (d, J = 7.2Hz, 4H); 13C NMR (CDCl3, 75MHz) δ: 21.2,123.9, 127.5, 127.6, 128.2, 137.9, 140.9*

4,4´-Dimethoxybiphenyl (2f)[64]**:** *White solid; mp 178-179^{0}C; 1H NMR ($CDCl_3$, 300 MHz) δ : 3.84 (s, 6H), 6.95 (dd, J = 4.8Hz, 6.9 Hz, 4H), 7.47 (dd, J = 4.8Hz, 6.9Hz, 4H); ^{13}C NMR ($CDCl_3$, 75 MHz) δ: 55.36, 114.1, 127.7, 133.4, 158.6.*

4,4´-Difluorobiphenyl (2g)[4]**:***White solid; mp 89-90^{0}C; ^{1}H NMR ($CDCl_3$, 300 MHz) δ : 7.09-7.15 (m, 4H), 7.46-7.51 (m, 4H); ^{13}C NMR ($CDCl_3$, 75 MHz) δ: 115.7(d, J= 21 Hz), 128.6(d, J = 8 Hz), 136.4(d, J = 4 Hz), 162.4 (d, J= 245 Hz).*

2,2´-Dichlorobiphenyl (2h)[15]**:***White solid; mp 60-62^{0}C; ^{1}H NMR ($CDCl_3$, 300 MHz) δ : 7.26-7.37 (m, 6H), 7.47-7.51 (m, 2H); ^{13}C NMR ($CDCl_3$, 75 MHz) δ: 126.4, 129.1, 129.3, 131.0, 133.4, 138.2.*

2,2´-Dibromobiphenyl (2i)[65]**:** *White solid; mp 79-81^{0}C; ^{1}H NMR ($CDCl_3$, 300 MHz) δ : 7.23-7.29 (m, 4H), 7.32-7.40 (m, 2H), 7,67 (d, J = 8.1Hz, 2H); ^{13}C NMR ($CDCl_3$, 75 MHz) δ: 123.5, 127.1, 129.4, 131.0, 132.6, 142.0.*

5,5´-Dichloro-2,2´-bithiophene (2j)[66]**:** *White solid; mp 107^{0}C; ^{1}H NMR ($CDCl_3$, 300 MHz) δ : 6.82 (d, J = 3.9 Hz, 2H), 6.85 (d, J = 3.6 Hz, 2H); ^{13}C NMR ($CDCl_3$, 75 MHz) δ: 122.9, 126.7, 129.1, 134.9.*

5,5´-Dimethyl-2,2´-bithiophene(2k)[67]**:** Yellow solid; mp 65-67^{0}C; ^{1}H NMR ($CDCl_3$, 300 MHz) δ : 2.46 (s, 6H), 6.63 (dd, *J* = 2.4Hz, 3.6Hz, 2H), 6.87 (d, *J* = 3.6Hz, 2H); ^{13}C NMR ($CDCl_3$, 75 MHz) δ: 15.3, 122.8, 125.7, 135.5, 138.4.

2,2´-dithiophene (2l)[64]**:** White solid; mp 33-34 °C; ^{1}H NMR ($CDCl_3$, 300 MHz,): δ 7.00-7.03 (m, 2 H), 7.18 (dd, *J* = 3.6 Hz, *J* = 1.2 Hz, 2 H), 7.22 (dd, *J* = 5.1 Hz, *J* = 0.9 Hz, 2 H); ^{13}C NMR (75 MHz, $CDCl_3$): δ 123.77, 124.36, 127.78, 137.40.

6,6´-Dimethoxy-3,3´-dipyridyl (2m)[68]**:** White solid; mp 105°C; ^{1}H NMR ($CDCl_3$, 300 MHz) δ : 3.98 (s, 6H), 6.84 (d, *J* = 8.4Hz, 2H), 7.73 (dd, *J* = 6Hz, 8.7Hz, 2H), 8.32 (d, *J* = 2.4Hz, 2H); ^{13}C NMR ($CDCl_3$, 75 MHz) δ: 53.7, 111.1, 126.9, 137.2, 144.3, 163.5.

1-Phenylnaphthalene (3a)[69]**:** Colorless liquid; ^{1}H NMR ($CDCl_3$, 300 MHz) δ: 7.39-7.54 (m, 9H), 7.84-7.91 (m, 3H); ^{13}C NMR ($CDCl_3$, 75 MHz) δ: 125.3, 125.7, 126.01, 126.03, 126.9, 127.2, 127.6, 128.2, 130, 131.6, 133.8, 140.2, 140.7, 145.6.

4-methoxybiphenyl (3b)[69]**:** White solid; mp 86^{0}C ^{1}H NMR ($CDCl_3$, 300 MHz) δ: 3.86 (s, 3H), 6.99 (dd, *J* = 2.1Hz, 6.9Hz, 2H), 7.27-7.34 (m, 1H), 7.40-7.45 (m, 2H), 7.53-7.58 (m,

4H); ^{13}C NMR ($CDCl_3$, 75 MHz) δ: 54.3, 113.2, 125.6, 125.7, 127.1, 127.7, 132.7, 139.8, 158.1.

3-Phenylquinoline (3c)[69]**:** Faint yellowish oil; ^{1}H NMR ($CDCl_3$, 300 MHz) δ: 7.25 (s, 1H), 7.41-7.61 (m, 3H), 7.69-7.76 (m, 3H), 7.89 (d, *J* = 7.8Hz, 1H), 8.16 (d, *J* = 8.4Hz, 1H), 8.32 (d, *J* = 2.1Hz, 1H), 9.22 (bs,1H); ^{13}C NMR ($CDCl_3$, 75MHz) δ: 127.1, 127.4, 128.0, 128.1, 129.0, 129.2, 129.5, 133.4, 133,9, 137.8.

4-cyanobiphenyl (3d)[70]**:** White solid; ^{1}H NMR ($CDCl_3$, 300MHz) δ: 7.64-7.71 (m, 4H), 7.55-7.59 (m, 2H), 7.38-7.50 (m, 3H); ^{13}C NMR ($CDCl_3$, 75 MHz) δ: 145.66, 139.16, 132. 62, 129.16, 128.71, 127.75, 127.25, 118.99, 110.91.

3-methylbiphenyl (3e)[71]**:** Isolated as a colorless liquid; ^{1}H NMR (300MHz, $CDCl_3$) δ: 7.69 (d, *J* = 8.7Hz, 2H),7.52 (m, 4H),7.43(m,2H), 7.26 (d, *J* = 7.2Hz,1H), 2.59 (s, 3H); ^{13}C NMR (75MHz, $CDCl_3$) δ: 141.5, 141.3, 138.4,128.9, 128.80,128.78,128.2,128.1,127.3,124.4, 21.6.

2-methylbiphenyl (3f)[8]**:** Colorless oil; ^{1}H NMR (300 MHz, $CDCl_3$) δ: 7.46-7.57 (m, 5H), 7.38-7.45 (m, 4H), 2.42 (s, 1H); ^{13}C NMR (75 MHz, $CDCl_3$) δ: 142.1, 141.4, 135.5, 130.5, 129.9, 129.3, 128.2, 127.4, 126.9, 125.9, 20.6.

4-Cyano-4'-formylbiphenyl (3g)[8]**:** Isolated as a white solid; ^{1}H NMR ($CDCl_3$, 300MHz) δ: 10.02 (s, 1H), 7.99 (d, *J* = 7.8 Hz, 2H), 7.72-7.79 (m, 6H); ^{13}C NMR (75 MHz, $CDCl_3$) δ: 191.7, 144.9, 144.1, 136.1, 132.8, 130.5, 128.1, 127.9, 118.6, 112.1.

3-(4-Fluro-phenyl)-quinoline (3h)[8]**:** Isolated as a white solid; ^{1}H NMR ($CDCl_3$, 300MHz) δ: 9.16 (d, *J* = 2.1Hz, 1H), 8.33 (d, *J* = 2.1Hz, 1H), 8.21 (d, *J*=8.4Hz,1H), 7.71-7.80 (m,1H), 7.60-7.71 (m, 4H), 7.23-7.28 (m,2H) ^{13}C NMR (75 MHz, $CDCl_3$) δ: 164.7,161.4,149.0(J_{CF} = 3.3Hz), 146.5, 134.1, 133.7 (J_{CF} = 7.4 Hz), 133.4, 133.0, 129.9, 129.5, 129.1 (J_{CF} = 8 Hz), 128.7, 128.0 (J_{CF} = 3.9 Hz), 127.2 (J_{CF} = 26.70 Hz), 116.3 (J_{CF} = 21.5 Hz).

2-fluorobiphenyl (3i)[72]**:** Isolated as a white solid; Isolated as white solid; ^{1}H NMR (300 MHz, $CDCl_3$) δ: 7.15-7.57 (m, 9H); ^{13}C NMR (75 MHz, $CDCl_3$) δ: 159.8 (J_{CF} = 246 Hz, CF), 135.8 (C_6H_5), 130.8 (J_{CF} = 3.6 Hz, CH), 129.2 (C_6H_5), 129.0 (J_{CF} = 3Hz, CH), 128.9 (C_6H_5), 128.7 (C_6H_5), 128.4 (C_6H_5), 127.4 (J_{CF} = 36 Hz, C_6H_5F), 124.3 (J_{CF}= 3.6 Hz, CH), 116.1 (J_{CF} = 22.5 Hz, CH).

3-chlorobiphenyl (3j)[73]**:** Isolated as colorless oil; ^{1}H NMR (300 MHz, $CDCl_3$) δ: 7.59-7.65 (m, 3H), 7.35-7.53 (m, 6H); ^{13}C NMR (75MHz, $CDCl_3$) δ: 143.1, 139.8, 134.7, 130.1, 129.0, 128.0, 127.4, 127.3, 127.2, 125.4.

1,3-Diphenylbenzene (3k)[8]**:** Isolated as white solid; ^{1}H NMR (300 MHz, $CDCl_3$) δ: 7.81 (m,1H), 7.65 (dd, *J* = 8.4Hz,1.5Hz, 4H), 7.55-7.61 (m, 2H), 7.54 (t, 1H), 7.46-7.49 (m, 3H),

7.44 (t, 1H), 7.35-7.40 (m, 2H); ^{13}C NMR (75 MHz, $CDCl_3$) δ: 141.8, 141.2, 129.2, 128.8, 127.4, 127.3,126.2, 126.1.

III.D.Summary

This report summarizes anionic, water/AOT/Cy RM as an efficient reaction medium for additive and ligand-free transition metal catalysed C-C homo/cross coupling reactions with a broad range of substrates compares to cationic (DDAB) and non-ionic (TX 100) RMs in cyclohexane under comparable physicochemical conditions. The reaction proceeds rapidly and completes within 10 mins at ambient condition. Performance of the reaction has been correlated with different physicochemical parameters of these self-organized media using conductance, DLS and FTIR techniques. A plausible explanation is suggested in favor of AOT/Cy RM to be an effective reaction medium in terms of yield of the final product. Subsequently, a series of studies were undertaken to find out a most suitable base and the influence of water content (ω) of this medium under optimized condition for effective C-C homocoupling reaction of arylboronic acid (herein, phenylboronic acid was selected as a model compound) which constitute a major part of this report. K_2CO_3 (91%) and Cs_2CO_3 (96%) have been found to be least and most effective base, respectively in terms of yield. Droplet size [in other words (ω)] influences the yield in studied ω range (5→20) and shows a maximum at ω equals to 15. The progress of the reaction in constrained environment of RM and the possible reaction site have also been assessed by employing conductance, DLS and FTIR techniques. The droplet core in nano-cage of RM, especially the bound water layer of RM gallows has been emphasized as the probable reaction site. Finally, it was explored for the construction of symmetrical and unsymmetrical biaryl *via* C-C bond forming homo/cross-coupling reaction (28 different entries) in AOT RM using same protocol. The yield of coupled products have been discussed in view of variation in electron withdrawing group in arylhalides (Cl^-, Br^- and I^-) and bond strength between C-halide. Investigations of other organic reactions in such promising micellar and RM media comprising single and mixed surfactant(s) are currently underway in our laboratory.

III.E.References

References are given in BIBLIOGRAPHY under Chapter-III (pp. 108-111).